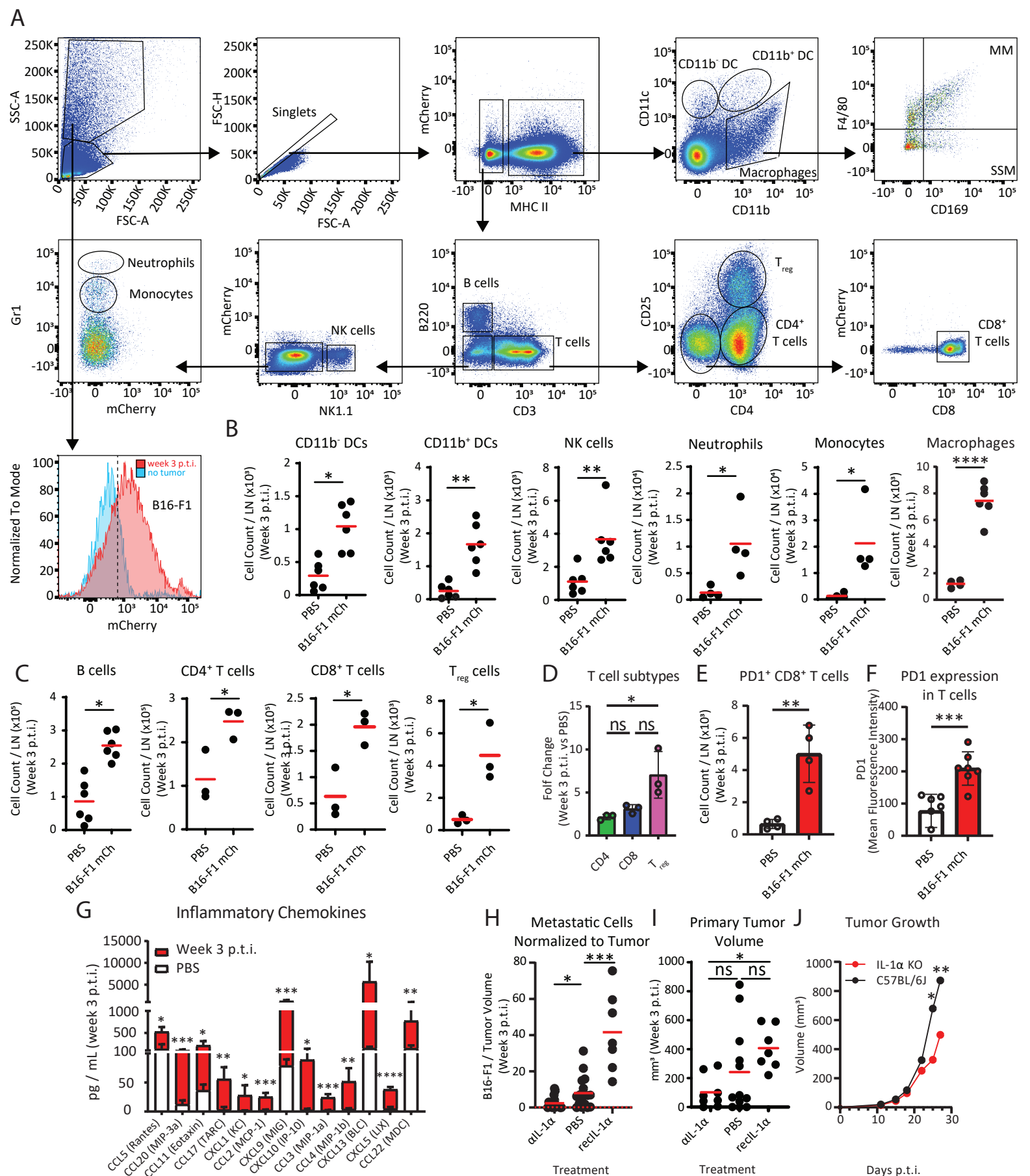


**Supplementary Figure 1 - Mouse melanoma metastases growth in the sentinel LN**

(A, left) Transmitted light and (A, right) mCherry microscope pictures of transduced B16-F1 mCherry.

(B) Representative pictures of primary tumor growth at week one, two and three p.t.i.. (C) Timecourse indicating tumor volume in the first three weeks p.t.i.. (D) Confocal micrograph showing sLN (left) at week three p.t.i. and

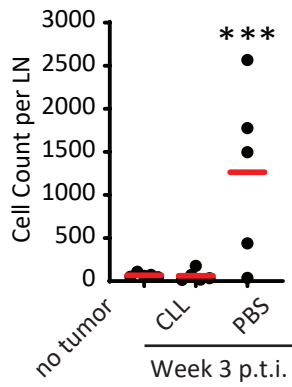
(right) magnification of the metastasis invading the SS and IF areas.



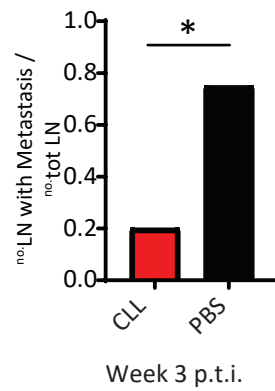
**Supplementary figure 2: Pro-tumoral release of IL-1 $\alpha$  in the metastatic LN**

(A) FACS gating strategy to detect immune cells. In addition to B16 melanoma (mCherry<sup>+</sup>), different cells are detectable from single cells, including CD11b<sup>-</sup> DCs (MHC II<sup>+</sup>, CD11c<sup>+</sup>, CD11b<sup>-</sup>), CD11b<sup>+</sup> DCs (MHC II<sup>+</sup>, CD11c<sup>+</sup>, CD11b<sup>+</sup>), subcapsular sinus macrophages (SSM, MHC II<sup>+</sup>, CD11c<sup>intlow</sup>, CD11b<sup>+</sup>, CD169<sup>+</sup>, F4/80<sup>+</sup>), medullary macrophages (MM, MHC II<sup>+</sup>, CD11c<sup>intlow</sup>, CD11b<sup>+</sup>, CD169<sup>+</sup>, F4/80<sup>+</sup>), B cells (MHC II<sup>+</sup>, CD3<sup>+</sup>, B220<sup>+</sup>), CD4<sup>+</sup> T cells (MHC II<sup>+</sup>, B220<sup>-</sup>, CD3<sup>+</sup>, CD4<sup>+</sup>, CD25<sup>-</sup>), T<sub>reg</sub> (MHC II<sup>+</sup>, B220<sup>-</sup>, CD3<sup>+</sup>, CD4<sup>+</sup>, CD25<sup>+</sup>), CD8<sup>+</sup> T cells (MHC II<sup>+</sup>, B220<sup>-</sup>, CD3<sup>+</sup>, CD4<sup>-</sup>, CD25<sup>-</sup>, CD8<sup>+</sup>), NK cells (MHC II<sup>+</sup>, B220<sup>-</sup>, CD3<sup>-</sup>, NK1.1<sup>+</sup>), neutrophils (MHC II<sup>+</sup>, B220<sup>-</sup>, CD3<sup>-</sup>, NK1.1<sup>+</sup>, Gr1<sup>high</sup>) and monocytes (MHC II<sup>+</sup>, B220<sup>-</sup>, CD3<sup>-</sup>, NK1.1<sup>-</sup>, Gr1<sup>int</sup>) and B16 melanoma (mCherry<sup>+</sup>). Quantification of the total number of (B) innate and (C) adaptive immune cells in metastatic sLN at week three p.t.i.. (D) Fold change increase of CD4<sup>+</sup>, CD8<sup>+</sup> and regulatory T cells in tumor in comparison to control. (E) Quantification of the number of PD1<sup>+</sup> cells and (F) PD1 mean expression in CD8<sup>+</sup> T cells at week three p.t.i. in comparison to controls. (G) Inflammatory chemokines in metastatic sLN (red) in comparison to mice without tumor (white). (H) Number of metastatic melanoma cells in the sLN in mice treated with anti IL-1 $\alpha$  or recombinant IL-1 $\alpha$ , normalized to the primary tumor volume. The red dashed line indicates the background, calculated on the number of events in non-tumor-bearing mice. (I) Primary tumor volume in mice treated with anti IL-1 $\alpha$  blocking antibody or with recombinant IL-1 $\alpha$  in comparison to untreated. (J) Primary tumor growth in IL-1 $\alpha$  wild type and IL-1 $\alpha$  KO mice.

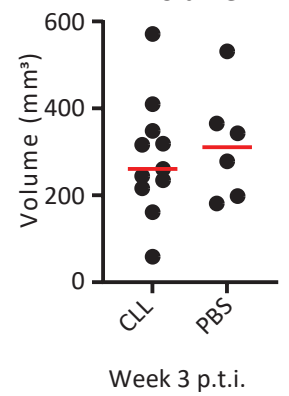
### A Metastatic Cells



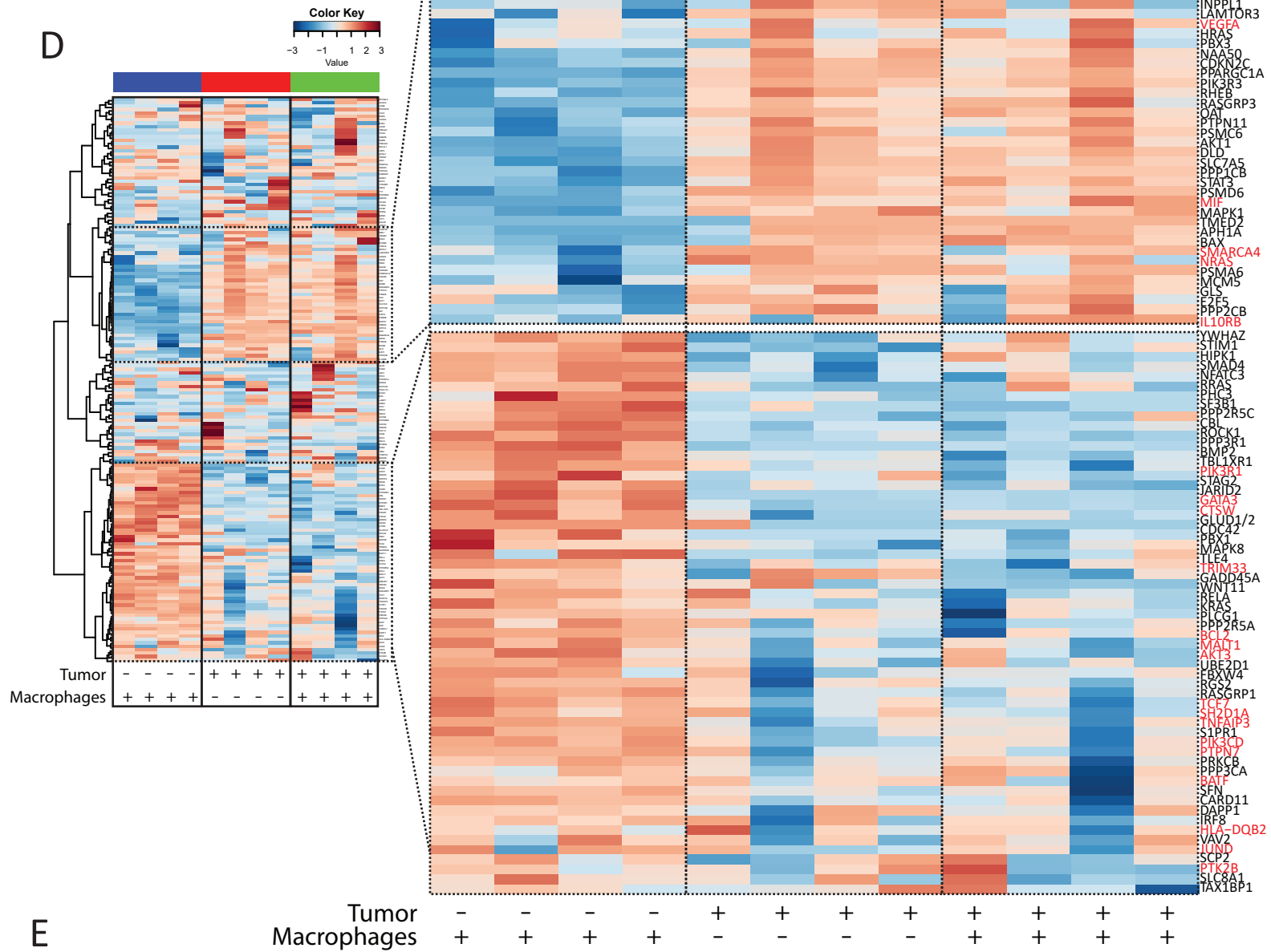
### B Metastatic Ratio



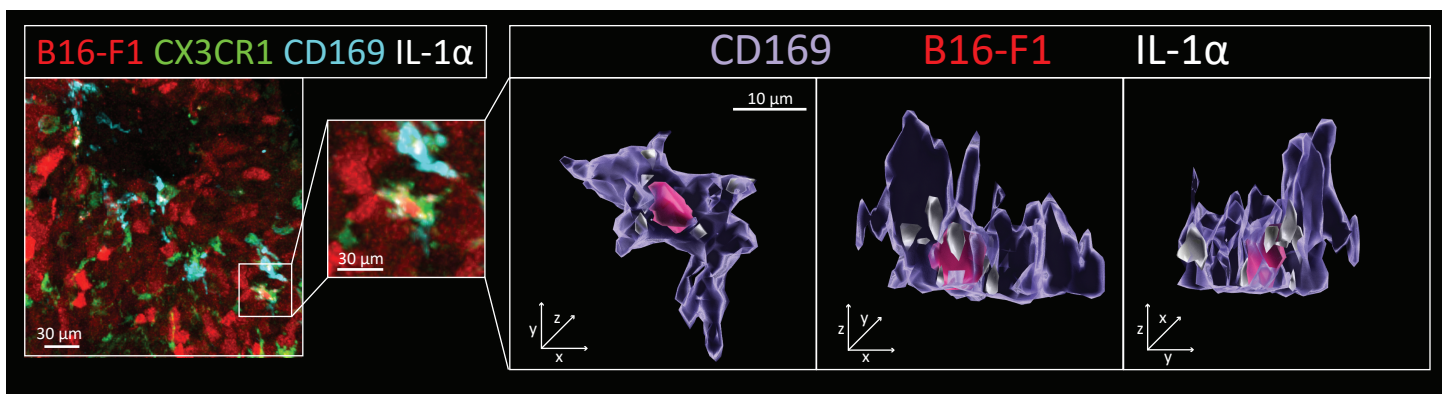
### C Primary Tumor Volume

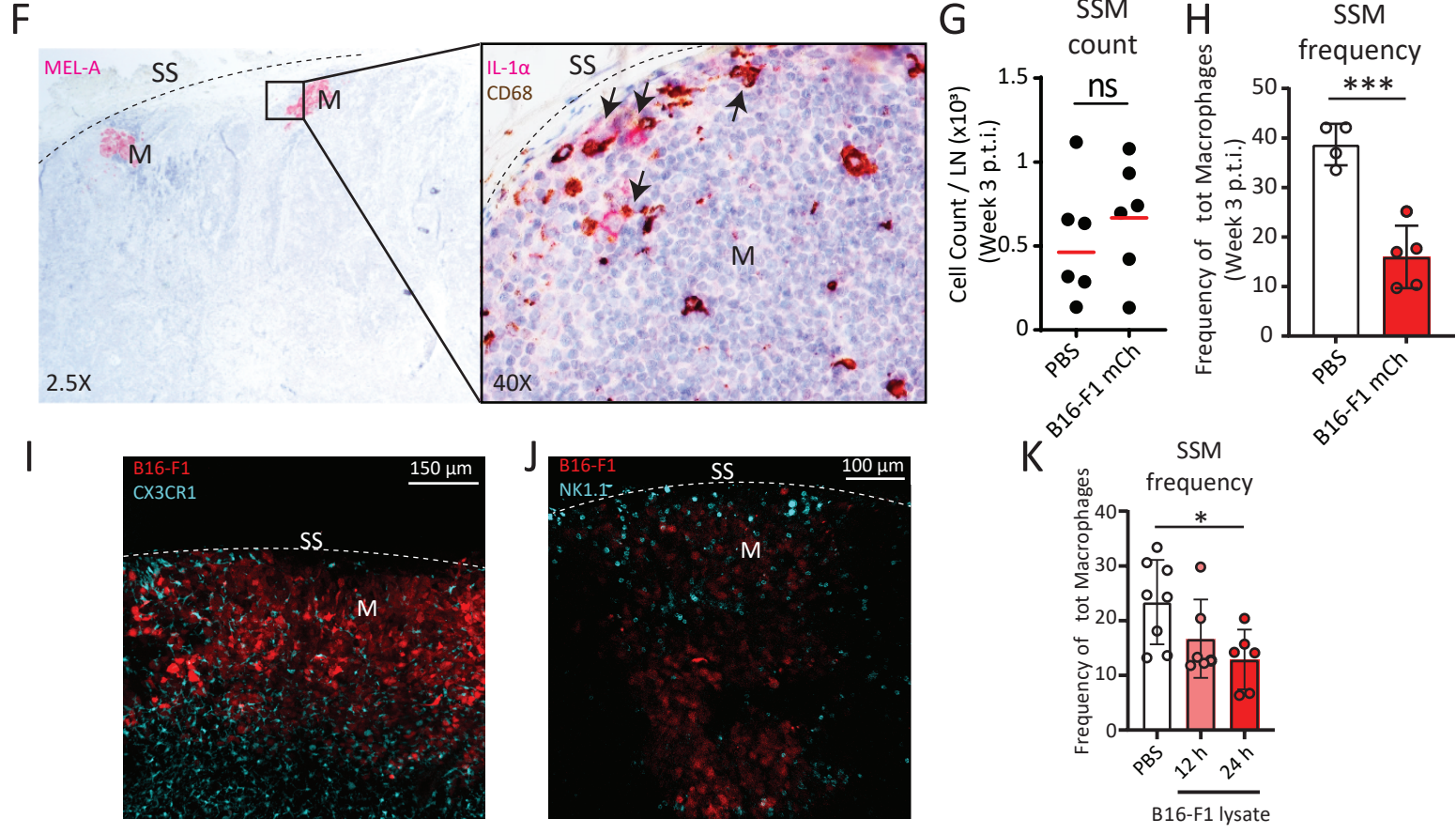


### D



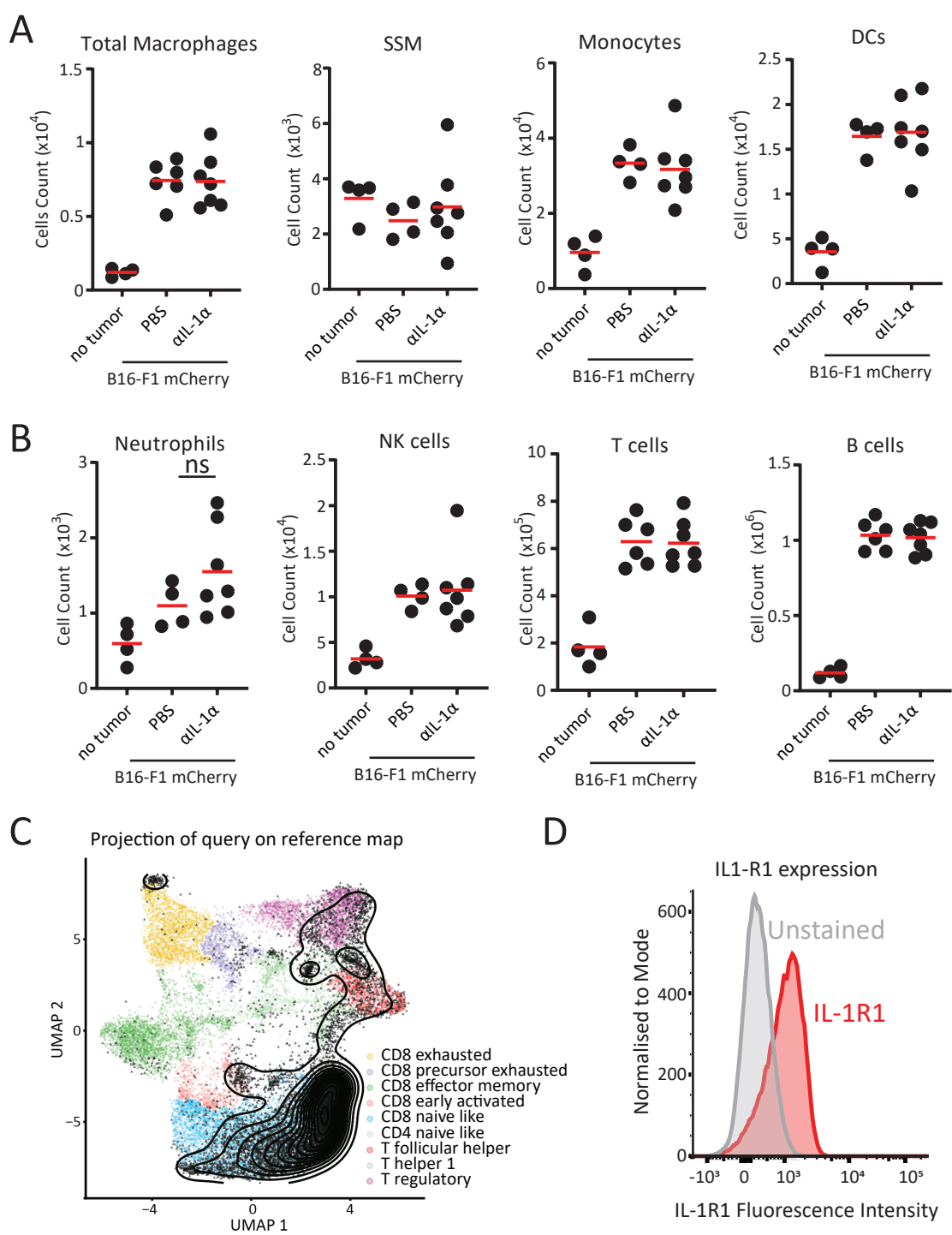
### E





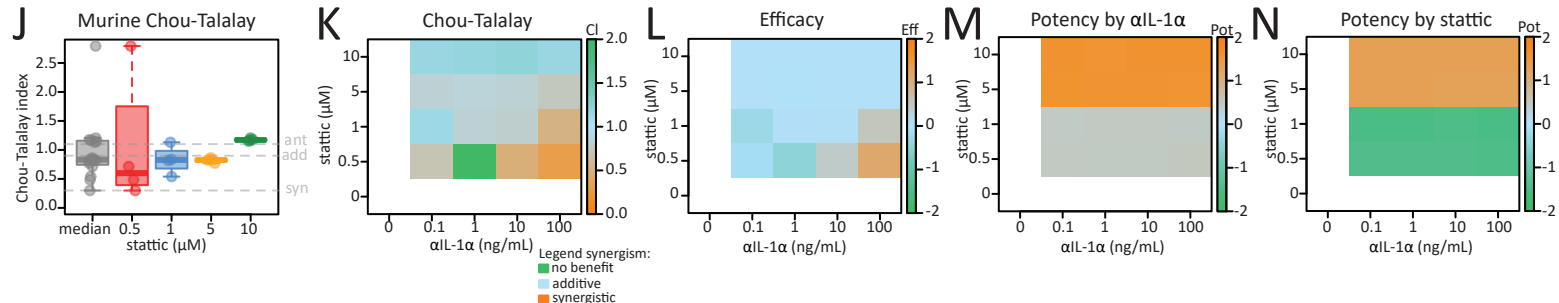
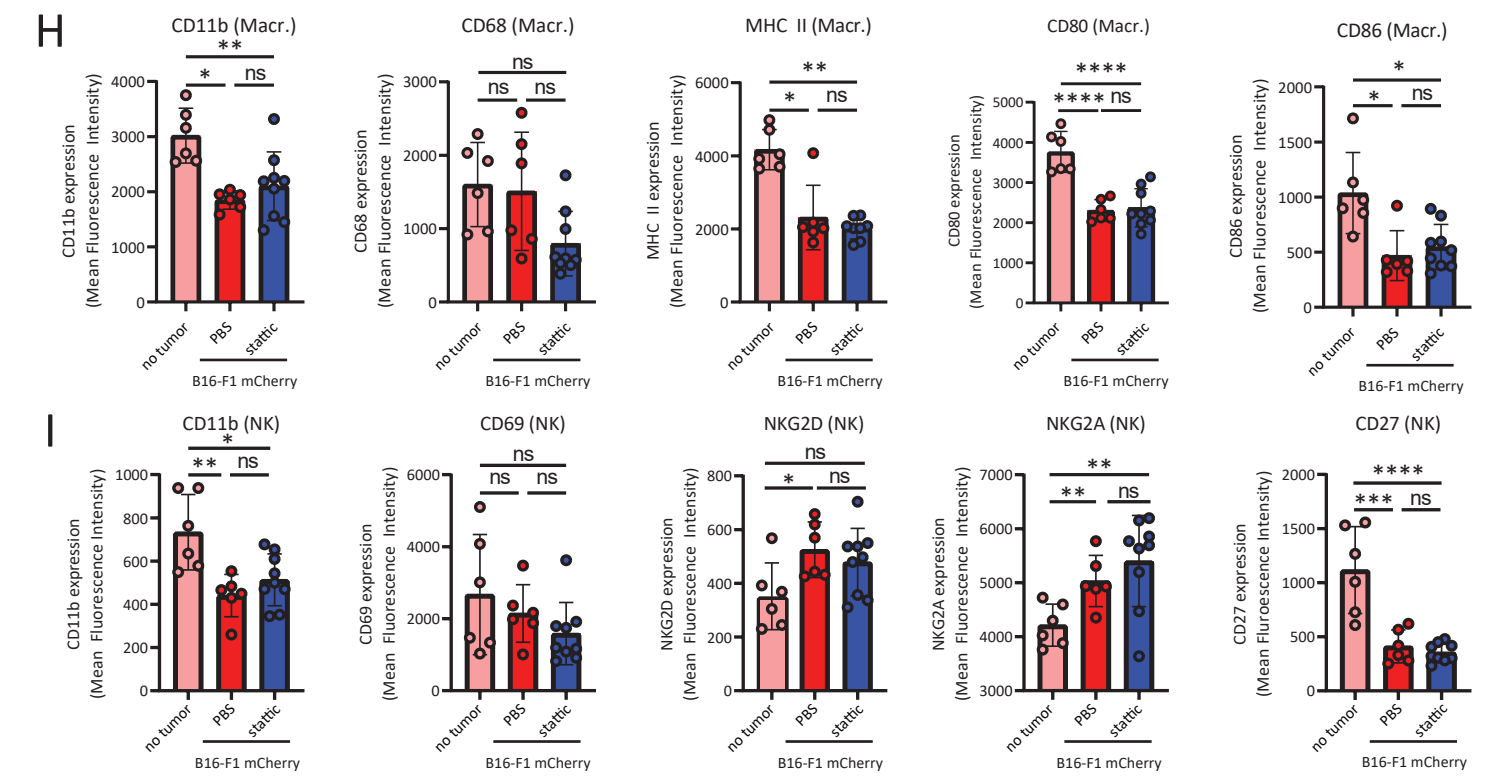
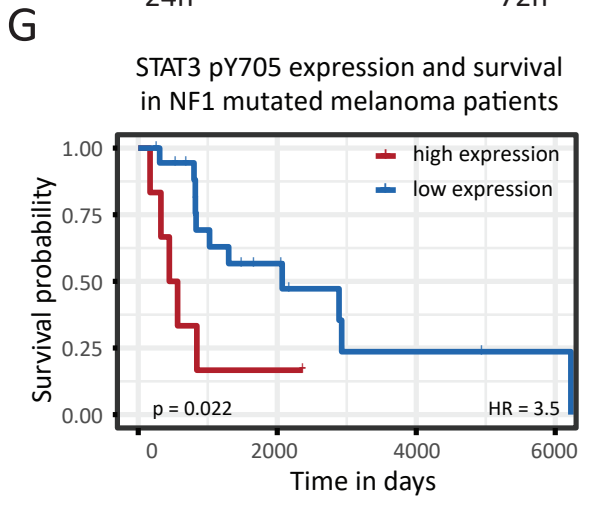
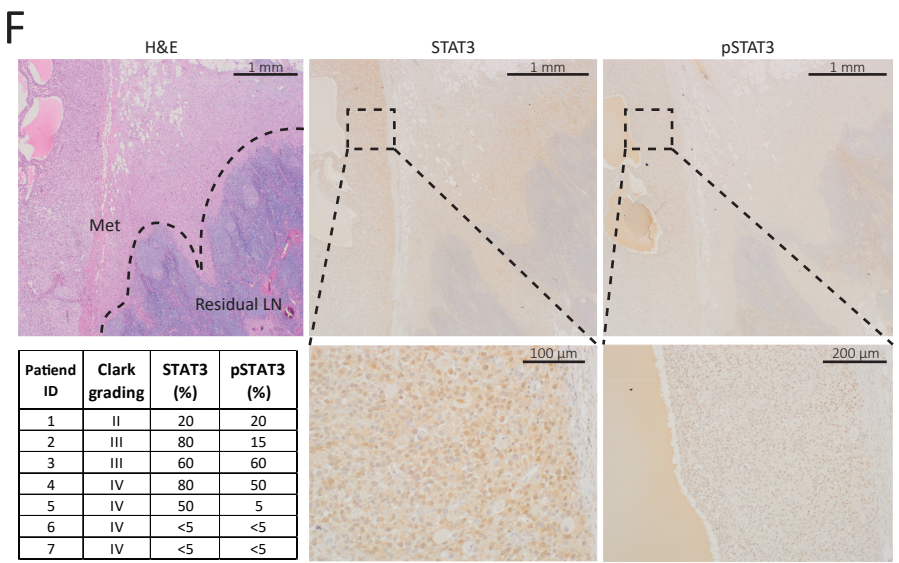
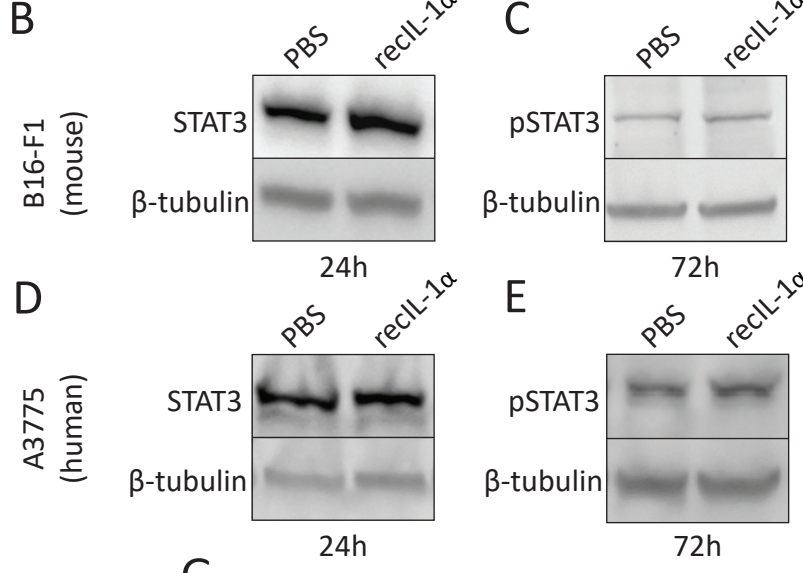
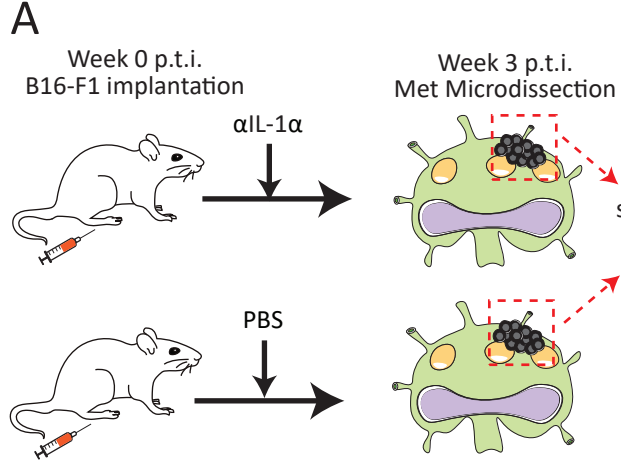
**Supplementary figure 3: SSM are the main source of IL-1 $\alpha$**

(A) Total number of metastatic cells in sLN of mice treated with clodronate liposomes (CLL) in comparison to negative controls. (B) Metastatic ratio and (C) Primary tumor volume in mice treated with CLL in comparison to untreated mice. (D, left) Heatmap representing average expression of genes related to immunosuppression and immune exhaustion in metastatic LN three weeks p.t.i. from mice depleted for macrophages (green) in comparison to untreated mice (red) and mice without tumor (blue). (D, right) Magnifications of two regions of the previous heatmap showing, highlighted in red, some relevant genes associated with immune suppression (above) and immune activation (below). (E, left) Confocal micrographs showing a tumor infiltrating SSM and (E, right) corresponding 3D reconstruction indicating intracellular accumulation of tumor (red) and IL-1 $\alpha$  (white). (F, left) Representative section of human sLN showing presence of melanoma metastases (pink), indicated with the letter M. (F, right) Magnification of metastatic area highlighting infiltration of CD68<sup>+</sup> macrophages (brown) and expression of IL-1 $\alpha$  (pink). Representative macrophages positive to IL-1 $\alpha$  are indicated by black arrows. (G) Total number of SSM and (H) frequency on total LN macrophages at three weeks p.t.i.. Confocal micrographs of metastasis infiltrated by (I) myeloid CX3CR1<sup>+</sup> cells and (J) NK cells. (K) Frequency of SSM at 12 and 24 hours after injection of tumor cell lysate.



**Supplementary figure 4: SSM derived IL-1 $\alpha$  directly supports tumor proliferation**

Total number of (A) phagocytic and (B) non phagocytic immune cells in sLN of mice treated with anti IL-1 $\alpha$  antibody in comparison to untreated at three weeks p.t.i.. (C) Projection of the T cell subsets identity on the scSeq UMAP map. (D) Expression of IL-1R1 in B16-F1 *in vitro*.



### Supplementary figure 5: IL-1 $\alpha$ induces STAT3 expression and phosphorylation in tumor

(A) Scheme representing the design of scSeq experiment. Representative immunoblot of (B) STAT3 and (C) pSTAT3 in murine melanoma and (D) STAT3 and (E) pSTAT3 in human melanoma. (F) Histological sections of a representative metastatic lesion in the sLN of a human patient, stained with haematoxylin and eosin (H&E, left) in comparison to IHC staining of STAT3 (center) and pSTAT3 (right), with corresponding magnifications (below). (F, below left) Table reporting Clark grading and percentage of STAT3 and pSTAT3 positive cells in 7 human metastatic sLN. (G) Survival probability of NF1 mutated melanoma patients according to high (red) or low (blue) expression of pSTAT3. Flow cytometric quantification of activation markers of (H) macrophages (CD11b, CD68, MHC II, CD80 and CD86) and (I) NK cells (CD11b, CD69, NKG2D, NKG2A and CD27), expressed as mean fluorescence intensity, in metastatic lesions of untreated mice in comparison to animals treated with the STAT3i stattic and mice without tumor. (J) Samples distribution of the Chou-Talalay Index of the combination therapy, indicating the thresholds for synergistic, additive and antagonist effect in grey. (K) Chou-Talalay Index, (L) efficacy, (M) potency by anti IL-1 $\alpha$ , and (N) potency by stattic of the combination therapy, all indicated as average expression of samples.